HHS Public Access

Author manuscript

Stem Cells. Author manuscript; available in PMC 2016 November 28.

Published in final edited form as:

Stem Cells. 2016 February ; 34(2): 405–417. doi:10.1002/stem.2235.

Ataxia Telangiectasia Mutated Dysregulation Results in Diabetic Retinopathy

Ashay D. Bhatwadekar[a,b], **Yaqian Duan**[a], **Harshini Chakravarthy**[c], **Maria Korah**[b], **Sergio Caballero**[b], **Julia V. Busik**[c], and **Maria B. Grant**[a,b]

[a]Department of Ophthalmology, Indiana University, Indianapolis, Indiana, USA

[b]Department of Pharmacology and Therapeutics, University of Florida, Florida, USA

[c]Department of Physiology, Michigan State University, East Lansing, Michigan

Abstract

Ataxia telangiectasia mutated (ATM) acts as a defense against a variety of bone marrow (BM) stressors. We hypothesized that ATM loss in BM-hematopoietic stem cells (HSCs) would be detrimental to both HSC function and microvascular repair while sustained ATM would be beneficial in disease models of diabetes. Chronic diabetes represents a condition associated with HSC depletion and inadequate vascular repair. Gender mismatched chimeras of $ATM^{-/-}$ on wild type background were generated and a cohort were made diabetic using streptozotocin (STZ). HSCs from the STZ-$ATM^{-/-}$chimeras showed (a) reduced self-renewal; (b) decreased long-term repopulation; (c) depletion from the primitive endosteal niche; (d) myeloid bias; and (e) accelerated diabetic retinopathy (DR). To further test the significance of ATM in hematopoiesis and diabetes, we performed microarrays on circulating angiogenic cells, $CD34^+$ cells, obtained from a unique cohort of human subjects with long-standing (>40 years duration) poorly controlled diabetes that were free of DR. Pathway analysis of microarrays in these individuals revealed DNA repair and cell-cycle regulation as the top networks with marked upregulation of ATM mRNA compared with $CD34^+$ cells from diabetics with DR. In conclusion, our study highlights using rodent models and human subjects, the critical role of ATM in microvascular repair in DR.

Keywords

Diabetic retinopathy; Ataxia telangiectasia mutated; Hematopoietic stem cells

Correspondence: Maria B. Grant, M.D., Department of Ophthalmology, Eugene and Marilyn Glick Eye Institute, 980 W Walnut Street, Indianapolis, Indiana 46203, USA. Telephone: 317-274-2628; Fax: 317-274-2277; mabgrant@iupui.edu; or Ashay Bhatwadekar, Ph.D., Department of Ophthalmology, Eugene and Marilyn Glick Eye Institute, 1160 W Michigan Street, GK-318, Indianapolis, Indiana 46202, USA. Telephone: 317-278-5075; Fax: 317-274-2277; abhatwad@iupui.edu.

Disclosure of Potential Conflicts of Interest

The authors indicate no potential conflicts of interest.

Author Contributions

A.D.B.: conception and design, data collection analysis and interpretation, manuscript writing, financial support; Y.D.: data collection, analysis and interpretation; H.C.: data collection; M.K.: data collection; S.C.: technical help with chimeric mice; J.V.B.: experimental design; M.B.G.: conception and design, manuscript writing, financial support, final approval.

Introduction

Diabetic retinopathy (DR), the most common of all the microvascular complications, is debilitating and is associated with progressive loss of endothelial cells and pericytes leading to widespread areas of vasodegeneration and subsequent non-perfusion [1, 2]. Unlike other microvascular beds of body, such as kidney or nerves, the retina faces a unique challenge in diabetes due to the combination of high metabolic demand and minimal vascular supply which limits the retina's ability to adapt to the metabolic stress of diabetes. The intricate network of vascular and neural cells, higher oxygen demand, and sparse vascularity makes the retina the most vulnerable to diabetic stress of all tissues [3]. The retina can lose as much as 38% of resident endothelial cells within 20 months of experimental diabetes [4].

DR is increasingly gaining momentum as the disease of the BM-origins. Studies performed on non-diabetic hematopoietic chimeras suggest a significant contribution of hemangioblast of BM-origin in repair and maintenance of retinal vasculature [5]. Almost 10% of endothelial cells in neo-vessels that developed in response to injury are BM-derived [6], indicating a critical role of the BM in repair. In DR, the retina experiences a deficiency of the reparative cells and invasion of inflammatory monocytes and macrophages occurs. The coordinated chemokine secretion and the involvement of retinal microglia, Muller cells and retinal pigment epithelium along with the infiltration by the BM-monocytes/macrophages further exacerbate retinopathy [7].Although several studies emphasize the identification of retinal cellular dysfunction, the role of diabetic BM microenvironment in repair and inflammation in DR remains largely unknown.

The BM microenvironment plays a crucial role in the process of hematopoietic stem cell (HSC) self-renewal, differentiation, and stem cell fate. A million mature blood cells are produced per second in the normal adult human BM. Under physiologic conditions there exist a perfect balance of this enormous demand yet there is preservation of an adequate pool of HSCs [8], demonstrating the well-orchestrated dynamics of self-renewal govern HSC demand and supply [9, 10]. The balance between self-renewal and differentiation is of critical importance as too little self-renewal can jeopardize the ability to sustain hematopoiesis throughout life while excessive differentiation can result in conditions such as leukemogenesis.

Normally HSCs give rise to 10% myeloid and 90% lymphoid type cells, however, with pathological conditions like diabetes or with physiological ageing this balance shifts towards more myeloid and fewer lymphoid cells creating a state of myeoloidosis [11]. Diabetic oxidative stress causes a rapid decline in the number of HSCs in the low perfused areas (endosteal niche) of BM which represents the home for the most primitive cells, the long-term repopulating (LTR)-HSCs. [12, 13]. Moreover, diabetes leads to elevated levels of oxidative DNA damage and decreased DNA repair[14].

Ataxia telangiectasia mutated (ATM), a tumor suppressor protein, is known to be activated in response to DNA damage and is responsible for regulating oxidative stress in HSCs [15]. ATM helps to correct DNA damage by activating downstream targets and leading to the recruitment of DNA repair proteins to the sites of DNA damage [16]. Diabetes leads to DNA

damage and decreased efficacy of DNA repair [14]. Interestingly, aged ATM$^{-/-}$ mice exhibit marked increase in blood glucose levels with a decrease in insulin and c-peptide levels while young ATM$^{-/-}$ display transient hyperglycemia during oral glucose challenge [17, 18].

Diabetes leads to a selective decline of LTR-HSCs from the well protected osteoblastic niche [13] and increase in inflammatory short-term repopulating (STR)-HSCs which may result in an increase in retinal permeability and increase in leukocyte trafficking, the early markers of DR [19–21]. The molecular regulators of HSC imbalance, however, have not been tested in any diabetic animal model system. We hypothesize that ATM is critical in harboring LTR-HSCs in BM and its loss in BM-HSCs would deplete vaso-reparative cells creating a proinflammatory phenotype both in retina and BM and accelerating DR pathology. We also hypothesize that maintaining ATM in diabetes would serve to protect the LTR-HSC and prevent development of DR.

Materials and Methods

Animals

All animal studies received a prior approval by the institutional animal care and use committee. The studies were conducted in accordance with The Guiding Principles in the Care and Use of Animals (NIH) as well as per the Association of Research in Vision and Ophthalmology (ARVO) Statement for the use of Animals in Ophthalmic and Vision Research. Wild type (WT) (C57BL/6J) and ATM$^{-/-}$ (B6.129S6-Atm^{tm1Awb}/J) mice of about 4 weeks old were purchased from the Jackson Laboratories (Bar Harbor, ME, https://www.jax.org/) and maintained at animal care facilities at the University of Florida. The animals received regular diet (Harlan, Tampa, FL, http://www.envigo.com/) during the study period. The animals had access to food and water ad libitum. At study termination, the animals were killed by overdose of ketamine and xylazine (14 and 30 mg/kg, respectively).

WT mice were made chimeric by replacing BM from ATM$^{-/-}$ and WT mice as described previously [5]. Briefly, WT mice were placed in a purpose built irradiator box and irradiated in the gamma source irradiator (800–900 rads) of animal care services at the University of Florida (ATM$^{-/-}$→WT group) and Michigan State University (WT→WT group) to inactivate the resident BM. Sca1 and c-kit cells were isolated from the femurs of ATM$^{-/-}$ mice (8 weeks old) and injected retro-orbitally in recipient mice.

Eight weeks after stable engraftment the mice were segregated in two groups; one group received STZ (IP at a dose of 40 mg/kg) to induce diabetes while the other group received vehicle and served as control. Six months after STZ treatment, the animals were killed and tissues were harvested for analysis. At study termination all the animals were about 9 months old.

Human Study

We re-analyzed data for human study from our previous study [22]. The study was approved by the Institutional Review Board at the University of Florida. The informed consent was obtained from study participants prior to withdrawal of blood samples. The following are brief details of the study design, additional details are provided in Supporting Information

section. We recruited diabetic individuals with >40 years of diabetes but were free of DR (n = 5), diabetic individuals age-, sex-, and metabolic control-matched with the previous group but with DR (n = 5) and control patients (n = 5) all age and sex matched. $CD34^+$ cells were isolated and the total RNA from CD34 cells was extracted and the cDNA was probed to Human RSTA Affymetrix 2.0 chip and the samples were run for gene expression profile using AffyNugen amplification protocol. The data were analyzed using Ingenuity Pathway Analysis (IPA) and Gene Set Enrichment Analysis (GSEA) [23].

Trypsin Digestion of Mouse Retina

Retinas were trypsin digested to enumerate number of acellu-lar capillaries as described [24]. Briefly, formalin fixed retinas were digested in 3% Trypsin 250 (BD-Difco, NJ, http://www.bd.com/ds/). Following incubation for 1.5–2 hours, the internal limiting membrane was carefully separated and digested. Retina was mounted on glass slides followed by staining with periodic acid-Schiff's base (PAS)-hematoxylin (Sigma-Aldrich St. Louis, MO, https://www.sigmaaldrich.com/united-states.html). The images were captured using Leica DM300 microscope. The acellular capillaries were evaluated in central to mid-peripheral areas between artery and vein. Using this approach for evaluation about 8–10 fields were captured and the number of acellular capillaries per square millimeter were quantified.

Quantitative Real-Time Polymerase Chain Reaction

Total RNA was isolated from snap frozen retinas using Trizol extraction (Invitrogen, https://www.thermofisher.com/us/en/home/brands/invitrogen.html) as per manufacturer's instructions. RNA (1 μg) was reverse transcribed using iScript c-DNA synthesis kit. mRNA expression for gene specific primers was determined using Taqman Gene Expression Assays (Applied Biosystems, Foster City, CA, http://www.thermofisher.com/us/en/home/brands/applied-bio-systems.html) on ViiA7 real-time polymerase chain reaction (PCR) system. Individual gene expressions were normalized to TATA-binding protein and expressed as relative gene expression.

BM Protein Estimation

BM was harvested by flushing with phosphate-buffered saline, following separation of cellular fraction the supernatant solution was concentrated using ultra-centrifugation filter units (Millipore, Bedford, MA, http://www.emdmillipore.com/). The concentrated fraction was analyzed for mouse cytokine array panel using Luminex bead-based immunoassay platform (Assaygate, Ijamsville, MD, http://www.assaygate.com/). The data were represented as pg of analyte per milligram of total protein.

Flow Cytometry

Isolated BM was treated with the following cocktail of antibodies to differentiate LTR and STR-HSCs: PerCpCy5.5 mouse lineage antibody cocktail, FITC rat anti-mouse CD34, PE-Cy7 rat anti-mouse sca1, and APC rat anti-mouse c-kit. The cell suspension was analyzed using LSR-II flow cytometer and data were analyzed using FCS Express analysis software.

Statistics

The data are represented as mean ± SEM. The statistical analysis was performed using one way analysis of variance (ANOVA) followed by post hoc Student's Newman Keul Test or Student's *t*-test or two way ANOVA followed by Bonferroni post-test using GraphPad Prism Software (La Jolla, CA, http://www.graph-pad.com/scientific-software/prism/). Mean difference of $p < 0.05$ was considered to be statistically significant.

Results

Metabolic Parameters

At sacrifice all the animals showed almost similar body weight. As expected the HbA_{1c} value for $ATM^{-/-}$→WT + STZ and WT + STZ mice was significantly higher ($p < 0.05$) when compared with WT and $ATM^{-/-}$→WT group. There was a twofold increase in monocytes for WT + STZ and $ATM^{-/-}$→WT + STZ group in comparison with WT and $ATM^{-/-}$→WT group, respectively ($p < 0.05$); Supporting Information Table 1.

LTR-HSCs and STR-HSCs Imbalance in Diabetes

To test the effect of BM exhaustion of LTR-HSCs on vascular repair of the retina, we developed gender mismatched chimeric mice which specifically lacked ATM in BM ($ATM^{-/-}$→WT). Mice were then segregated in two groups; one group was treated with STZ to induce type 1 diabetes while the other group served as the vehicle control. Mice were euthanized at 24 weeks and the BM was analyzed to determine the levels of LTR-HSCs and of short-term repopulating HSC (STR-HSCs). Figure 1A shows a representative schematic of dot plots used for flow cytometry analysis. $Lin^{-}Sca1^{+}$ $ckit^{+}$ $CD34^{-}$ cells were identified as LTR-HSCs and$Lin^{-}Sca1^{+}$ $ckit^{+}$ $CD34^{+}$ as STR-HSCs, respectively. STZ-induced diabetes resulted in a 1.8-fold decrease ($p < 0.01$) in LTR-HSCs when compared with WT mice. BM-specific loss of ATM (i.e., $ATM^{-/-}$→WT group) resulted in a 1.3-fold decrease; however, this difference was statistically insignificant. STZ treatment of $ATM^{-/-}$→WT intensified this defect resulting in a fourfold decrease in LTR-HSCs when compared with control $ATM^{-/-}$→WT and WT + STZ animals (Fig. 1B).

Diabetes represents a state of chronic inflammation with an increase in myeloid biased STR-HSCs and with a decrease in LTR-HSCs [25]. To test this hypothesis in the ATM-chimeras with experimental DR, the ratio of STR-HSCs to LTR-HSCs was determined. A 1.6-fold increase in the ratio of STR-HSCs to LTR-HSCs was detected in the STZ group when compared with WT group ($p < 0.05$).The diabetic $ATM^{-/-}$→WT group showed a profound imbalance indicating a significant increase in STR-HSCs likely due to the combined deleterious effect of diabetes and loss of ATM expression (Fig. 1C).

Overall, the $ATM^{-/-}$→WT + STZ group showed marked decrease in LTR-HSCs with an increase in STR-HSCs, suggesting that lack ATM in BM is necessary to maintain LTR-STR balance and that this is lost during diabetes.

Decrease in Cell Quiescence in Diabetic HSCs

Previous studies suggest that loss of ATM expression results in rapid progression of HSCs into the cell cycle [26]. To test this, LTR-HSCs and STR-HSCs were stained with Pyronin Y and Hoechst Blue and then analyzed using flow cytometry. Approximately 25% of LTR-HSCs of WT animals were quiescent with approximately 75% of cells in active G2 stage. Diabetes lead to a 50% decrease in LTR-HSCs with a 12% increase in number of cells in G2 phase ($p < 0.05$). Diabetes with ATM depletion forced the entire population into the active phase of the cell cycle ($p < 0.05$), indicating total loss of quiescent LTR-HSCs for BM rejuvenation (Fig. 2).

Similar to the above, diabetes resulted in a profound decrease in quiescent STR-HSCs ($p < 0.05$) when compared with WT controls. Both groups of ATM chimeric mice showed almost all cell populations in an active stage of cell cycling.

Alteration of Cell Cycle Check Points in ATM Chimeras

To understand the mechanism of BM exhaustion, cell pellets for mRNA determination were prepared from BM cells and BM supernatants and were used for cytokine measurements. A sixfold increase ($p < 0.001$) in mRNA expression of *p53* was observed in diabetic mice while the *p53* expression was reduced by approximately fourfold ($p < 0.001$) in diabetic ATM chimeras (Fig. 3). There was an increase in *P21* expression in the diabetic $ATM^{-/-}\rightarrow$WT group when compared with the other groups ($p < 0.01$). There was no change in expression of *CDK2* and *CDC25a* (Fig. 3, middle panel).

ATM is known to regulate oxidative stress in BM-HSCs; to test this, mRNA expression of *SOD1* and *SOD2* was determined in BM-cells. A threefold ($p < 0.01$) increase in *SOD1* expression was observed after STZ treatment. The $ATM^{-/-}\rightarrow$WT group showed a 2.5-fold ($p < 0.05$) increase when compared with control while there was decrease in *SOD1* expression in the diabetic $ATM^{-/-}\rightarrow$WT group. For *SOD2*, the $ATM^{-/-}\rightarrow$WT group showed a twofold increase when compared with WT and diabetic animals; however, this did not reach statistical significance (Fig. 3, bottom panel).

Upregulation of Inflammatory Markers ATM Chimeras

Cytokine analysis of BM supernatants showed a profound increase in expression of Granulocyte macrophage colony-stimulating factor (GM-CSF), Macrophage colony-stimulating factor (M-CSF), interleukin (IL)-6, IL-23 ($p < 0.05$), and tumor necrosis factor (TNF)-alpha ($p < 0.05$) in the $ATM^{-/-}\rightarrow$WT group when compared with the WT animals, Supporting Information Figure 1A–1C. Unexpectedly, considering overall inflammatory status of diabetes, STZ-treated mice did not show a change in the above cytokines except for an increase in monocyte chemotactic protein 5 (MCP-5) and Granulocyte-colony stimulating factor (G-CSF). Moreover, STZ treatment of $ATM^{-/-}\rightarrow$WT mice did not result in any further change in cytokine expression, unlike the accelerated decrease in LTR-HSC shown in Figure 1B. Together, this suggests that loss of ATM regulation in BM poses a dual impact: (a) increase in cytokine production and (b) decrease in LTR-HSCs. However, diabetes selectively impacts LTR-HSCs while not changing cytokine expression.

Decrease in BM-HSC Engraftment and Selective Decline of LTR-HSCs from BM Niche

To determine the engraftment of LTR-HSCs and the specificity of the donor derived cells, quantitative real-time PCR (qRT-PCR) for SRY gene (sex determining region Y protein) which selectively targets Y chromosome positive cells was performed. While the engraftment for WT→WT animals was about 98% this number was reduced to 52% in the $ATM^{-/-}$→WT group. This diabetic group showed slightly higher engraftment of $ATM^{-/-}$ cells, we believe that the increase in engraftment for diabetic $ATM^{-/-}$→WT mice may be due to changes in BM microenvironment associated with diabetes. The percentage of engraftment for individual animal is shown in Supporting Information Figure 2.

Next, demineralized femurs were stained for *n*-cadherin to delineate the endosteal niche (LTR-HSCs) (Fig. 4A) whereas VE-cadherin was used to label osteoblast cells and sinusoidal niche (STR-HSCs) (Fig. 4B). To eliminate any effect of BM irradiation per se and STZ diabetes two additional control groups (WT→WT and WT→WT + STZ) were also evaluated for numbers of LTR and STR-HSCs.

$Sca1^{+}$ cells (green) in these niches were enumerated and a 1.5-fold ($p < 0.001$) decrease in LTR-HSCs was observed in endosteal niche after STZ treatment. A similar decrease was also observed in LTR-HSC numbers in $ATM^{-/-}$→WT group when compared with the WT animals ($p < 0.01$).The WT and WT→WT groups were not statistically different; however, there was a significant difference between LTR-HSCs for WT→WT and WT→WT + STZ mice ($p < 0.001$). The $ATM^{-/-}$→WT showed approximately twofold decrease in LTR-HSCs when compared with WT→WT group ($p < 0.001$). The $ATM^{-/-}$→WT group made diabetic showed profound decrease in LTR-HSCs in endosteal niche and the LTR-HSC number fell fourfold ($p < 0.01$) when compared with WT→WT animals while a twofold when compared with $ATM^{-/-}$→ WT group (Fig. 4A).

To determine the myeloid bias (similar to Fig. 1C), we enumerated $Sca1^{+}$ cells in sinusoidal niche and determined the ratio of STR to LTR-HSCs. While WT→ WT group did not differ significantly with the WT group, there was a statistically significant difference between the ratio of STR to LTR-HSCs in the WT→WT vs., WT→WT + STZ group ($p < 0.01$). We observed a 1.5-fold increase ($p < 0.05$) in ratio of STR/LTR HSC numbers for $ATM^{-/-}$→ WT + STZ mice when compared with WT→WT ($p < 0.001$), WT→WT + STZ ($p < 0.001$) and $ATM^{-/-}$ →WT ($p < 0.01$) groups suggesting myeloid biased differentiation of HSCs with diabetes (Fig. 4B).

Accelerated Increase in Acellular Capillaries and Dissociation of Occluding Junctions in Diabetic ATM Chimeras

To determine whether the imbalance in STR and LTR-HSCs and the increase in BM inflammation observed in the $ATM^{-/-}$→WT impacts vascular repair, trypsin digestion of retinas was performed and the vasculature was stained using PAS-hematoxylin (Fig. 5A). Enumeration of acellular capillaries, a pathologic hallmark of DR, revealed a 1.5-fold increase ($p < 0.01$) in the diabetic group when compared with the vehicle control group. The WT→WT group was not significantly different in number of acellular capillaries when compared with WT group, however, the number of acellular capillaries showed a significant

difference when compared with WT→WT + STZ group ($p < 0.05$). The $ATM^{-/-}$→WT + STZ mice showed profound increase in acellular capillaries when compared with both WT→WT + STZ ($p < 0.001$) and $ATM^{-/-}$→WT ($p < 0.001$) mice.

To test the effect of $ATM^{-/-}$ donor cells on severity of DR (i.e., number of acellular capillaries) the engrafted donor cells were correlated to the number of acellular capillaries. A positive correlation was observed between engrafted $ATM^{-/-}$ cells and number of acellular capillaries for $ATM^{-/-}$→WT + STZ group. No correlation was observed for acellular capillaries and donor cells in the $ATM^{-/-}$→WT group, Supporting Information Figure 3.

Previous studies suggest that diabetes results in decrease in local distribution and expression of tight junctional protein occludin [27]. To test this, we stained trypsin digested retinas with occludin. In WT mice, we observed occludin reactivity at the vessel borders with punctate staining (Supporting Information Fig. 4; white arrows), characteristic of intact junctional complex. In diabetic animals the overall occludin immune reactivity was reduced with loss of junctional integrity (the red arrows in Supporting Information Fig. 4 are highlighting discontinuous pattern of occludin staining). The tight junctional integrity was relatively intact for $ATM^{-/-}$→WT mice; however, there was profound decrease in immunoreactivity for $ATM^{-/-}$→WT + STZ mice

Loss of ATM Expression in BM Cells Increases Retinal Inflammation

To study whether the decline of LTR-HSCs and increase in STR-HSCs contribute to key targets of retinal vascular function and inflammation mRNA expression of the key markers, *vascular endothelial growth factor (VEGF), PDGF-β, HIF-1α, Glial fibrillary acidic protein (GFAP), CD45, CCL2, Lipocalin-2 (LCN-2)*, was determined. The relative mRNA expression was determined after normalizing Ct values of WT + STZ,WT→WT + STZ and ATM →WT + STZ groups to WT, WT→WT and ATM→WT + STZ group, respectively. The loss of ATM expression ($ATM^{-/-}$→WT) and diabetes in BM-cells ($ATM^{-/-}$→WT+ STZ) resulted in significant decrease in VEGF ($p < 0.01$) and PDGF-β ($p < 0.05$) expression while there was an increase in inflammatory makers such as HIF-1α ($p < 0.01$), GFAP ($p < 0.01$), CD45 ($p < 0.01$), and LCN-2 ($p < 0.01$); however, CCL2 did not reach significance (Fig. 6).

Optimum ATM Expression in $CD34^+$ Cells Protect from DR in Diabetic Individuals

Our hypothesis predicts that diabetic individuals that maintained ATM expression would maintain HSC levels and function and would thus be protected from DR. We identified a unique cohort of diabetic individuals which in spite of long-standing diabetes of >40 years duration remained free from developing DR (diabetes w/o DR). We postulated that the enhanced repair due to sustained levels of BM LTR-HSCs would be critical for preservation of vascular repair in these protected individuals. To test the above hypothesis, human $CD34^+$ (equivalent to murine HSCs) isolated from DM individuals without DR were matched to diabetics with DR (mild to severe non-proliferative DR [NPDR] ($n = 3$); proliferative DR [PDR]) and age-matched controls. Microarrays were performed on the RNA of $CD34^+$ cells isolated from these three cohorts. The microarray data were submitted to GEO (#GSE43950)

and published previously [22]. The data were first analyzed using IPA software and bar chart was generated for transcripts mapping top pathways. The P53 pathway which is involved in DNA repair response was mapped as top ninth pathway (Supporting Information Fig. 5; blue box). The P53 pathway was expanded further to explore different targets (Supporting Information Fig. 6; red box). ATM was selected as candidate molecule for our studies based on important role of ATM in DNA damage response.

The data were further analyzed using a GSEA analysis [23, 28]. The data set was enriched for c2 curated gene sets involving 1320 canonical pathways. A distinct signature was observed for diabetic individuals, clearly separating controls from the diabetics. Top 50 down and upregulated transcripts are summarized on a heat map in Figure 7A. When diabetic individuals with DR (diabetes w/DR) were compared with diabetic individuals without DR (diabetes w/o DR), 173 of 1048 gene sets were upregulated in the diabetes w/o DR cohort while 875/1048 gene sets are upregulated in the diabetes w/DR cohort. Top 50 transcripts up/downrgulated in individuals between these groups are summarized in Figure 7B. Canonical pathway analysis revealed 17% mapping of gene sets in group with diabetes w/oDR while remaining 83% gene sets were mapped in diabetic individuals with DR (Supporting Information Fig. 7A).The “cell cycle pathway” mapped the highest percentage of gene sets with a substantial percentage of pathways involving transcripts for cell cycle and DNA repair (red bars; Supporting Information Fig. 7B). Diabetes w/oDR group showed a positive correlation with both cell cycle pathway (Supporting Information Fig. 8A) and p53 signaling pathway (Supporting Information Fig. 8B). To validate microarray data, qRT-PCR from the $CD34^+$ cells isolated from above three groups was performed. A fivefold increase ($p < 0.05$) in an expression of *ATM* was observed in individuals who were protected from developing DR when compared with individuals who developed DR (Fig. 7C).

Discussion

This study identified for the first time ATM as the critical regulator responsible for maintaining HSC balance during the development of DR, thus adding a new dimension to current understanding of pathogenic mechanisms of DR. In our clinical study, using a unique cohort of diabetic individuals protected from DR, we show the importance of optimum levels of ATM for defense against vascular damage of diabetes. Furthermore, this study highlights the importance of BM rejuvenation for vascular repair during diabetes.

It is well-established in animal models that long-standing diabetes leads to DR. A variety of mechanisms including inflammation, oxidative stress, and an increase in cytokines are suggested as causative in pathogenesis of DR. These studies have mainly focused on retinal endothelial cells or pericytes and have not examined the mechanism of BM-failure. We used ATM chimeras to address this problem which enabled us to study both retinal cellular involvement and BM-failure in one model of DR.

We observed that loss of ATM regulation in diabetes not only resulted in a profound decrease in LTR-HSCs but also reduced HSC self-renewal causing an imbalance in STR/LTR-HSC ratio. Furthermore, our study suggests that the accelerated increase in acellular capillaries is the result of a selective decline in LTR-HSCs from the endosteal niche and the

overall increase in myeloidosis and inflammation of the BM as well as the retina. These findings are in agreement with a previous report [16] which showed a specific decrease in LTR-HSCs of ATM$^{-/-}$ chimeric mice.

While not directly tested in our study, we surmise that BM failure in ATM$^{-/-}$→WT chimeras is due to a decreased proliferative potential and the failure of long-term reconstitution of HSCs [16].We previously reported that long-term diabetes show progressive decline in progenitor cell population form 4 to 11 months of diabetes [21]. Oikawa et al. showed that diabetes results in decline in LTR-HSCs in endosteal niche with an increase in STR-HSCs in sinusoidal niche [12, 13], we observed similar changes due to diabetes, moreover in our study loss of ATM resulted in a marked acceleration in this decline of LTR-HSCs and a further increase in STR-HSCs. While we did not measure the recruitment of hemangioblast to the retina, we believe that the alteration of the reparative potential of these progenitors leads to defective cells that are incapable of repair and can adversely influence the resident vasculature by differentiating into myeloid cells.

The BM-microenvironment plays a crucial role in HSC self-renewal, differentiation and the ultimate fate of HSCs [29]. HSC self-renewal is not fully understood, but recent studies demonstrate the importance of cell cycle, apoptosis and oxidative stress response in establishing HSC homeostasis [30]. Under physiological hematopoietic cell homeostasis, HSCs are one of the longest-lived cells due to their ability to maintain low levels of reactive oxygen species (ROS) [15, 31]. ATM is known to be activated in response to DNA damage and is essential in regulating oxidative stress in BM-HSCs and in maintaining their optimum levels in the BM [16, 32]. We observed an increase in expression of anti-oxidant enzymes, SOD1 and SOD2 supporting the critical role of oxidative stress in maintenance of long-term survival of HSCs and protection from DR.

The mechanism by which ATM serves to maintain the BM-HSC balance may involve an ATM partner, the fork head box-O-3 (FoxO3).The functional interaction between FoxO3 and ATM helps to counteract the DNA damage by activating downstream targets such as DNA damage inducible gene 45 (Gadd45) [15]. We observed an increase in Gadd45G in individuals protected from DR (Fig. 7B) suggesting the potential involvement of DNA damage response in this study and downstream involvement on anti-oxidant defense mechanisms. Conditional deletion of FoxO1, FoxO3, and FoxO4 isoforms in HSCs results in an HSC imbalance similar to that observed in this study [33].

Under steady state conditions with no hematologic insult, the majority of HSCs enter cell cycle infrequently [34]. ATM regulates HSC stem cell cycling and self-renewal both by ROS independent and dependent pathways mediated through p53 and p21.ATM activation enhances p53 expression and the loss of ATM reduces p53 expression [35]. We observed a decrease in p53 in both ATM chimeric groups. p53 is essential for cell cycle arrest and anti-oxidative stress functions of ATM. p53 directly activates a variety of downstream targets like SOD2, Fas-ligand, Gadd45, and p21. Interestingly, we observed an increase in p21 mRNA in BM cells which is suggestive of HSC quiescence. However, our cell cycle data do not support this assertion; however, we believe that this finding is mainly attributed to our use of the whole BM-fraction for mRNA analysis.

One of the major findings of our study is the proinflammatory phenotype in ATM$^{-/-}$→WT chimeric mice. We observed inflammation in BM and retina of these chimeric mice. Numerous reports have highlighted the importance of retinal inflammation in the pathogenesis of DR, similarly we observed an increase in the expression ofCD45, LCN-2, and GFAP [4, 36]. An upregulation of CD45 expression suggests global increase in retinal inflammation. While we saw a trend towards an increase in retinal CCL2, the increase did not achieve statistical significance. CCL-2 is needed for recruitment of macrophages/ microglia to the site of injury [37]. GFAP is known marker of Muller cell gliosis which is known to be activated in DR suggesting Muller cell inflammation in our animal model. An increase in LCN-2 which is produced by Muller cells and known to be expressed exclusively in inner retina undergoing neurovascular degeneration in DR [38] further supports above assertion of increase in gliosis in diabetic ATM$^{-/-}$ →WT mice.

An increase in retinal inflammation is also related to BM-inflammation as an increase in inflammatory markers such as GM-CSF, G-CSF, and TNF-α, as well as an increase in IL-23 is observed. Previous studies document that ATM acts as a repressor for IL-23 and that a decrease in ATM expression leads to increase in IL-23 expression. Typically IL-23 secretion is largely restricted to antigen presenting cells (APC), including monocyte-derived dendritic cells, myeloid DC, macrophage, and microglia in response to immune danger. Our study identifies for the first time, the novel role of IL-23 in BM inflammation and progression of DR [39].

DR begins with the loss of two important cellular components, that is, pericytes and the endothelial cells [40]. The enumeration of acellular capillaries is the most relevant morphological feature to assess the degree of retinopathy because it combines multiple mechanisms involving endothelial cells, pericytes, the extracellular matrix and the microenvironment components [41, 42]. Capitalizing on this critical assay of DR, our study indicate that ATM$^{-/-}$→ WT mice show an accelerated increase in acellular capillaries. A variety of molecular regulators are implicated in pathogenesis of DR. In agreement with previous studies, we observed a decrease in PDGF-β expression [43] with an increase in HIF-1α [44]. Despite the increase in HIF-1α, VEGF mRNA levels did not significantly increase [45] when compared with WT→WT + STZ group suggesting predominance of inflammatory mechanisms in development of acellular capillaries in our studies.

In this study, we demonstrate the critical role of ATM maintenance in the clinical setting by using a unique cohort of diabetic individuals protected from DR. We have previously reported that this patient population showed an increase in the protective arm of the renin-angiotensin axis (Ang1-7 and MAS1) and decease in TGF-β1 expression [46]. This study identifies a novel mechanism of protection of CD34^{+} cells from diabetic stress by recognizing the critical role of ATM in the long-term survival of HSCs. We believe that HSCs of these individuals maintained quiescence and low oxidative stress enabling the active participation of HSC in vascular repair and thus preventing the development of the vasodegenerative stage of DR.

Microvascular complications are the major cause of morbidity and mortality among diabetic patients. Most of the microvascular beds (e.g., kidney, large nerves, etc.) are affected in

diabetes but those in the retina exhibit the most significant pathology due to the sparse vascularity and high metabolic demands of the retina. Cellular therapy to revascularize the microvasculature is promising but has limitations including the likely need for repetitive injections. Thus, there is an apparent lack of endogenous repair as well as limitations for autologous cell therapy to rebuild the injured microvasculature. Our study has opened a novel therapeutic option of BM rejuvenation for the repair of the injured retina and paves a way for developing BM centric targeted drug delivery for the treatment of DR.

Conclusions

Our study suggests for the first time the critical role of ATM in protecting BM-HSCs from the metabolic stress of diabetes and highlights the importance of maintaining LTR-HSCs for retinal vascular repair in DR. Our human diabetic studies support that maintenance of ATM expression protects HSCs providing a sustained source of HSCs for vascular repair.

Supplementary Material

Refer to Web version on PubMed Central for supplementary material.

Acknowledgments

We thank Dr. Tom A. Gardiner, Queen's University Belfast, for helpful discussion in designing experiments, Dr. Eleni Beli, Indiana University, for her help with flow-cytometry analysis, and Dr. Sandra O'Reilly and MMD-Collaborative in vivo Metabolic core at MSU for generation of WT→WT chimeric mice. This work was supported by Thomas H Maren Junior Investigator Award (to A.D.B.); Grants NIH R01HL11017-03, NEI R01EY007739-23, R01EY012601-15, and NIDDK R01DK090730-04 (to M.B.G.); and by unrestricted award from Research to Prevent Blindness (RPB) foundation to Department of Ophthalmology, Indiana University.

References

1. Engerman RL. Pathogenesis of diabetic retinopathy. Diabetes. 1989; 38:1203–1206. [PubMed: 2676655]
2. Kowluru RA, Chan PS. Oxidative stress and diabetic retinopathy. Exp Diabetes Res. 2007; 2007:43603. [PubMed: 17641741]
3. Curtis TM, Gardiner TA, Stitt AW. Microvascular lesions of diabetic retinopathy: Clues towards understanding pathogenesis? Eye (Lond). 2009; 23:1496–1508. [PubMed: 19444297]
4. Joussen AM, Doehmen S, Le ML, et al. TNF-alpha mediated apoptosis plays an important role in the development of early diabetic retinopathy and long-term histopathological alterations. Mol Vis. 2009; 15:1418–1428. [PubMed: 19641635]
5. Grant MB, May WS, Caballero S, et al. Adult hematopoietic stem cells provide functional hemangioblast activity during retinal neovascularization. Nat Med. 2002; 8:607–612. [PubMed: 12042812]
6. Wang C, Seifert RA, Bowen-Pope DF, et al. Diabetes and aging alter bone marrow contributions to tissue maintenance. Int J Physiol Pathophysiol Pharmacol. 2009; 2:20–28. [PubMed: 21383894]
7. Rutar M, Natoli R, Chia R, et al. Chemokine-mediated inflammation in the degenerating retina is coordinated by Muller cells, activated microglia, and retinal pigment epithelium. J Neuroinflammat. 2015; 12:8.
8. Seita J, Weissman IL. Hematopoietic stem cell: Self-renewal versus differentiation. Syst Biol Med. 2010; 2:640–653.
9. Stein MI, Zhu J, Emerson SG. Molecular pathways regulating the self-renewal of hematopoietic stem cells. Exp Hematol. 2004; 32:1129–1136. [PubMed: 15588937]

10. Eliasson P, Jonsson JI. The hematopoietic stem cell niche: Low in oxygen but a nice place to be. J Cell Physiol. 2010; 222:17–22. [PubMed: 19725055]
11. Muller-Sieburg C, Sieburg HB. Stem cell aging: Survival of the laziest? Cell cycle. 2008; 7:3798–3804. [PubMed: 19066464]
12. Orlandi A, Chavakis E, Seeger F, et al. Long-term diabetes impairs repopulation of hematopoietic progenitor cells and dysregulates the cytokine expression in the bone marrow microenvironment in mice. Basic Res Cardiol. 2010
13. Oikawa A, Siragusa M, Quaini F, et al. Diabetes mellitus induces bone marrow microangiopathy. Arterioscler Thromb Vasc Biol. 2010; 30:498–508. [PubMed: 20042708]
14. Blasiak J, Arabski M, Krupa R, et al. DNA damage and repair in type 2 diabetes mellitus. Mutat Res. 2004; 554:297–304. [PubMed: 15450427]
15. Yalcin S, Zhang X, Luciano JP, et al. Foxo3 is essential for the regulation of ataxia telangiectasia mutated and oxidative stress-mediated homeostasis of hematopoietic stem cells. J Biol Chem. 2008; 283:25692–25705. [PubMed: 18424439]
16. Ito K, Hirao A, Arai F, et al. Regulation of oxidative stress by ATM is required for self-renewal of haematopoietic stem cells. Nature. 2004; 431:997–1002. [PubMed: 15496926]
17. Miles PD, Treuner K, Latronica M, et al. Impaired insulin secretion in a mouse model of ataxia telangiectasia. Am J Physiol Endocrinol Metab. 2007; 293:E70–74. [PubMed: 17356010]
18. Barlow C, Hirotsune S, Paylor R, et al. Atm-deficient mice: A paradigm of ataxia telangiectasia. Cell. 1996; 86:159–171. [PubMed: 8689683]
19. Rojas M, Zhang W, Xu Z, et al. Requirement of NOX2 expression in both retina and bone marrow for diabetes-induced retinal vascular injury. PLoS One. 2013; 8:e84357. [PubMed: 24358357]
20. Li G, Veenstra AA, Talahalli RR, et al. Marrow-derived cells regulate the development of early diabetic retinopathy and tactile allodynia in mice. Diabetes. 2012; 61:3294–3303. [PubMed: 22923475]
21. Hazra S, Jarajapu YP, Stepps V, et al. Long-term type 1 diabetes influences haematopoietic stem cells by reducing vascular repair potential and increasing inflammatory monocyte generation in a murine model. Diabetologia. 2013; 56:644–653. [PubMed: 23192694]
22. Jarajapu YP, Bhatwadekar AD, Caballero S, et al. Activation of the ACE2/angiotensin-(1-7)/Mas receptor axis enhances the reparative function of dysfunctional diabetic endothelial progenitors. Diabetes. 2013; 62:1258–1269. [PubMed: 23230080]
23. Subramanian A, Tamayo P, Mootha VK, et al. Gene set enrichment analysis: A knowledge-based approach for interpreting genome-wide expression profiles. Proc Natl Acad Sci U S A. 2005; 102:15545–15550. [PubMed: 16199517]
24. Bhatwadekar A, Glenn JV, Figarola JL, et al. A new advanced glycation inhibitor, LR-90, prevents experimental diabetic retinopathy in rats. Br J Ophthalmol. 2008; 92:545–547. [PubMed: 18211931]
25. Chiba H, Ataka K, Iba K, et al. Diabetes impairs the interactions between long-term hematopoietic stem cells and osteopontin-positive cells in the endosteal niche of mouse bone marrow. Am J Physiol Cell Physiol. 2013; 305:C693–703. [PubMed: 23885062]
26. Morgan SE, Kastan MB. p53 and ATM: Cell cycle, cell death, and cancer. Advances in cancer research. 1997; 71:1–25. [PubMed: 9111862]
27. Barber AJ, Antonetti DA, Gardner TW. Altered expression of retinal occludin and glial fibrillary acidic protein in experimental diabetes. The Penn State Retina Research Group. Invest Ophthalmol Vis Sci. 2000; 41:3561–3568. [PubMed: 11006253]
28. Mootha VK, Lindgren CM, Eriksson KF, et al. PGC-1alpha-responsive genes involved in oxidative phosphorylation are coordinately downregulated in human diabetes. Nat Genet. 2003; 34:267–273. [PubMed: 12808457]
29. Ambrogini E, Almeida M, Martin-Millan M, et al. FoxO-mediated defense against oxidative stress in osteoblasts is indispensable for skeletal homeostasis in mice. Cell Metab. 2010; 11:136–146. [PubMed: 20142101]
30. Forsberg EC, Prohaska SS, Katzman S, et al. Differential expression of novel potential regulators in hematopoietic stem cells. PLoS Genet. 2005; 1:e28. [PubMed: 16151515]

31. Tothova Z, Gilliland DG. FoxO transcription factors and stem cell homeostasis: Insights from the hematopoietic system. Cell Stem Cell. 2007; 1:140–152. [PubMed: 18371346]
32. Barzilai A, Rotman G, Shiloh Y. ATM deficiency and oxidative stress: A new dimension of defective response to DNA damage. DNA Repair. 2002; 1:3–25. [PubMed: 12509294]
33. Tothova Z, Kollipara R, Huntly BJ, et al. FoxOs are critical mediators of hematopoietic stem cell resistance to physiologic oxidative stress. Cell. 2007; 128:325–339. [PubMed: 17254970]
34. Tipping AJ, Pina C, Castor A, et al. High GATA-2 expression inhibits human hematopoietic stem and progenitor cell function by effects on cell cycle. Blood. 2009; 113:2661–2672. [PubMed: 19168794]
35. Tsai WB, Chung YM, Takahashi Y, et al. Functional interaction between FOXO3a and ATM regulates DNA damage response. Nat Cell Biol. 2008; 10:460–467. [PubMed: 18344987]
36. Wilkinson-Berka JL, Alousis NS, Kelly DJ, et al. COX-2 inhibition and retinal angiogenesis in a mouse model of retinopathy of prematurity. Invest Ophthalmol Vis Sci. 2003; 44:974–979. [PubMed: 12601017]
37. Kuziel WA, Morgan SJ, Dawson TC, et al. Severe reduction in leukocyte adhesion and monocyte extravasation in mice deficient in CC chemokine receptor 2. Proc Natl Acad Sci U S A. 1997; 94:12053–12058. [PubMed: 9342361]
38. Kolibabka MWC, Busch S, Margerie D, Hammes HP, Molema G. Lipocalin-2 in degenerative Retinopathy. Diabetologie und Stoffwechsel. 2015; 10:P76.
39. Wang Q, Franks HA, Lax SJ, et al. The ataxia telangiectasia mutated kinase pathway regulates IL-23 expression by human dendritic cells. J Immunol. 2013; 190:3246–3255. [PubMed: 23460736]
40. Kern TS, Engerman RL. A mouse model of diabetic retinopathy. Arch Ophthalmol. 1996; 114:986–990. [PubMed: 8694735]
41. Hammes HP, Lin J, Renner O, et al. Pericytes and the pathogenesis of diabetic retinopathy. Diabetes. 2002; 51:3107–3112. [PubMed: 12351455]
42. Hammes HP, Feng Y, Pfister F, et al. Diabetic retinopathy: Targeting vasoregression. Diabetes. 2011; 60:9–16. [PubMed: 21193734]
43. Cox OT, Simpson DA, Stitt AW, et al. Sources of PDGF expression in murine retina and the effect of short-term diabetes. Mol Vis. 2003; 9:665–672. [PubMed: 14685146]
44. Lin M, Chen Y, Jin J, et al. Ischaemia-induced retinal neovascularisation and diabetic retinopathy in mice with conditional knockout of hypoxia-inducible factor-1 in retinal Muller cells. Diabetologia. 2011; 54:1554–1566. [PubMed: 21360191]
45. Gilbert RE, Vranes D, Berka JL, et al. Vascular endothelial growth factor and its receptors in control and diabetic rat eyes. Lab Invest. 1998; 78:1017–1027. [PubMed: 9714188]
46. Hazra S, Stepps V, Bhatwadekar AD, et al. Enhancing the function of CD34(+) cells by targeting plasminogen activator inhibitor-1. PloS one. 2013; 8:e79067. [PubMed: 24223881]

Significance Statement

The role of bone marrow (BM) derived circulating cells has garnered attention in the pathogenesis of diabetic retinopathy. Chronic diabetes represents a condition associated with hematopoietic stem cell (HSC) depletion and inadequate vascular repair. We test the hypothesis that loss of Ataxia telangiectasia mutated (ATM) in BM-HSCs would be detrimental to both HSC function and microvascular repair in the retina, while sustained expression of ATM would be beneficial. Our study findings indicate that maintaining optimum ATM expression is required for robust retinal microvascular repair and that ATM may serve as a critical target for BM rejuvenation in diabetes.

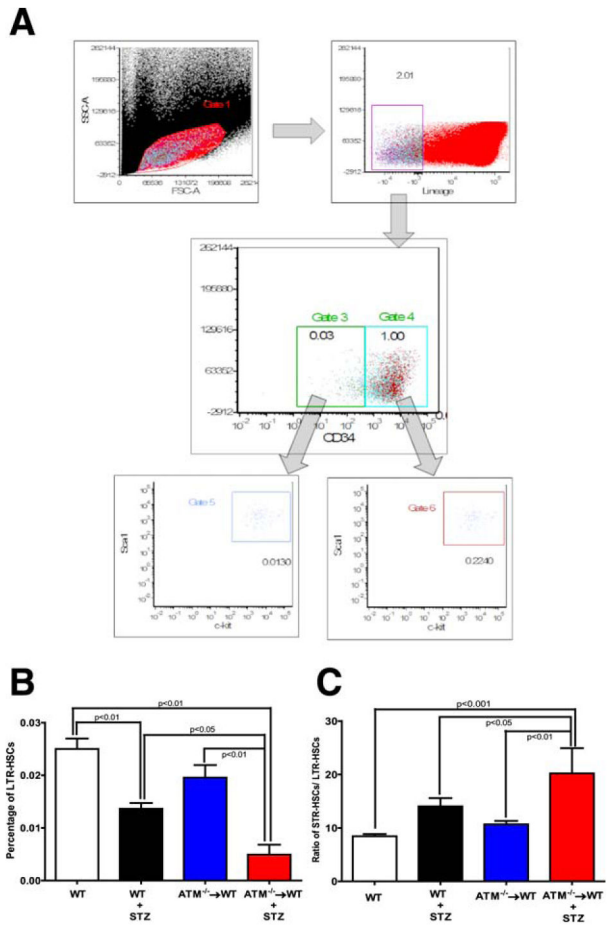

Figure 1.

Hematopoietic stem cell (HSC) imbalance in diabetic ataxia telangiectasia mutated $(ATM)^{-/-}\rightarrow$ wild type (WT) chimeras. **(A)**: Representative scheme for flow cytomtery dot plot used to differentiate and quantify long-term repopulating (LTR) and short-term repopulating (STR)-HSCs. $Lin^{-}Scal1^{+}$ c-kit^{+} $CD34^{-}$ and $Lin^{-}Scal1^{+}$ c-kit^{+} $CD34^{+}$ were identified as LTR-HSCs and STR-HSCs, respectively. Bar chart showing a quantification of **(B)** LTR-HSCs and **(C)** STR-HSCs. WT ($n = 12$), WT+ STZ ($n = 5$), $ATM^{-/-}\rightarrow WT$ ($n = 5$), $ATM^{-/-}\rightarrow WT$ ($n = 5$). Statistical test one way analysis of variance followed by Student's Newman Keul Test. Abbreviations: ATM, ataxia telangiectasia mutated; FSCA, forward-scattered light area; HSC, hematopoietic stem cell; LTR, long-term repopulating; SSCA, side-scattered light area; STZ, streptozotocin; WT, wild type.

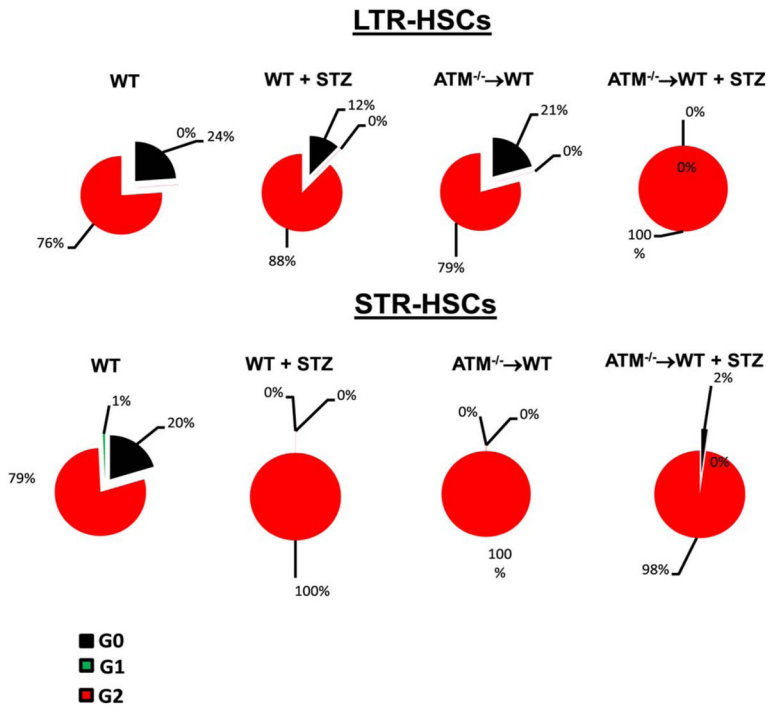

Figure 2.

Decrease in quiescent long-term repopulating (LTR)-hematopoietic stem cells (HSCs) and short-term repopulating (STR)-HSCs in ataxia telangiectasia mutated (ATM)$^{-/-}$→ wild type (WT) mice. Cell cycle status for LTR and STR-HSCs was determined following staining with Pyronin Y and Hoechst blue. Top panel showing a pie chart for the percentage of LTR-HSCs in different stages of cell cycle; diabetes and ATM$^{-/-}$→WT caused a significant decrease in quiescent (G0) LTR-HSCs with an increase in the numbers of cells in active cell cycle (G1 and G2). Bottom panel showing a significant lack in quiescent cells with an increase in cell numbers in the phase of the active cycle in all three groups except wild type (WT) animals. WT (n = 12), WT+ STZ (n = 5), ATM$^{-/-}$→WT (n = 5), ATM$^{-/-}$→WT (n = 5) Statistical test-one way analysis of variance followed by Student's Newman Keul Test. Abbreviations: ATM, ataxia telangiectasia mutated; HSC, hematopoietic stem cell; LTR, long-term repopulating; STR, short-term repopulating; STZ, streptozotocin; WT, wild type.

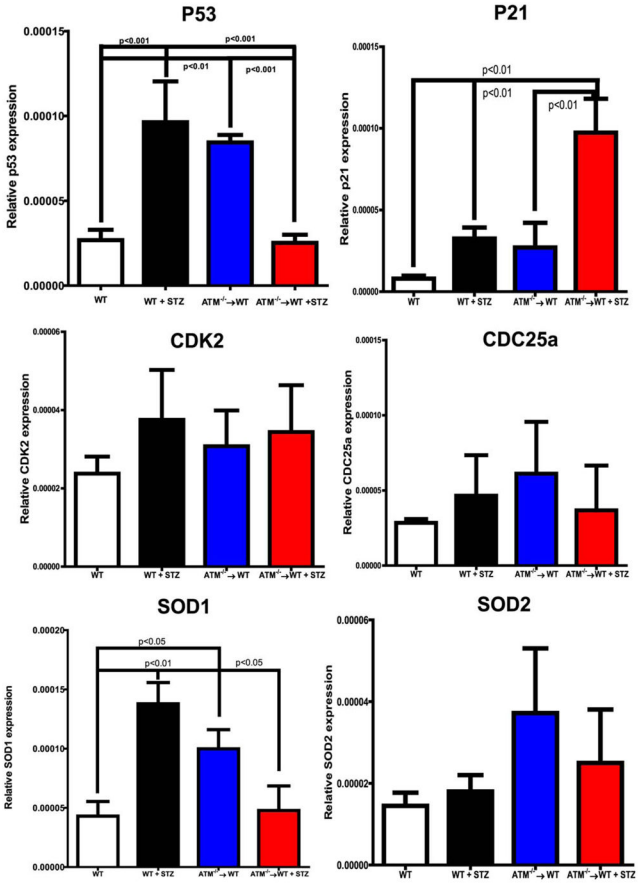

Figure 3.

mRNA expression of cell cycle check points and anti-oxidant enzymes in bone marrow cells. mRNA expression on bone marrow cell pellet was determined using q-RT-PCR. Bar chart showing expression of *P53*, *P21*, *CDK2*, *CDC25a*, *SOD1* and *SOD2*. Wild type (WT) (n = 4), WT+ STZ (n = 4), ataxia telangiectasia mutated (ATM)$^{-/-}$→WT (n = 5), ATM$^{-/-}$→WT (n = 5). Statistical Test- One way analysis of variance followed by Student's Newman Keul Test. Abbreviations: ATM, ataxia telangiectasia mutated; SOD, Superoxide dismutase; STZ, streptozotocin; WT, wild type.

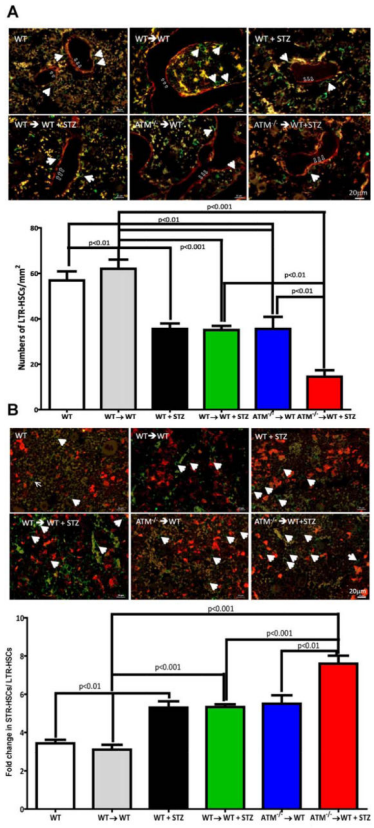

Figure 4.

Reduced bone marrow engraftment in diabetic ataxia telangiectasia mutated (ATM)$^{-/-}$→wild type (WT) chimeras. **(A)**: Demineralized mouse femurs were stained for *n*-cadherin (red) and c-kit (green) antibodies to identify long-term repopulating (LTR)-hematopoietic stem cells (HSCs). Representative photomicrographs from respective groups showing c-kit positive cells (white arrows) in an endosteal niche (open arrow) while bar chart showing a quantification of LTR-HSCs. **(B)**: Mouse femurs stained with ve-cadherin (red) to define the vascular niche. c-kit^{+} cells (white arrows) in ve-cadherin positive regions identified as short-term repopulating (STR)-HSC. Bar chart showing ratio of STR-HSCs to LTR-HSCs. Scale bar = 20 μm. WT (n = 6), WT→WT (n = 4), WT+ STZ (n = 5), WT→WT + STZ (n = 7), ATM$^{-/-}$→WT (n = 5), ATM$^{-/-}$→WT (n = 5). Statistical Test-One way analysis of variance followed by Student's Newman Keul Test. Abbreviations: ATM, ataxia telangiectasia mutated; HSC, hematopoietic stem cell; LTR, long-term repopulating; STZ, streptozotocin; WT, wild type.

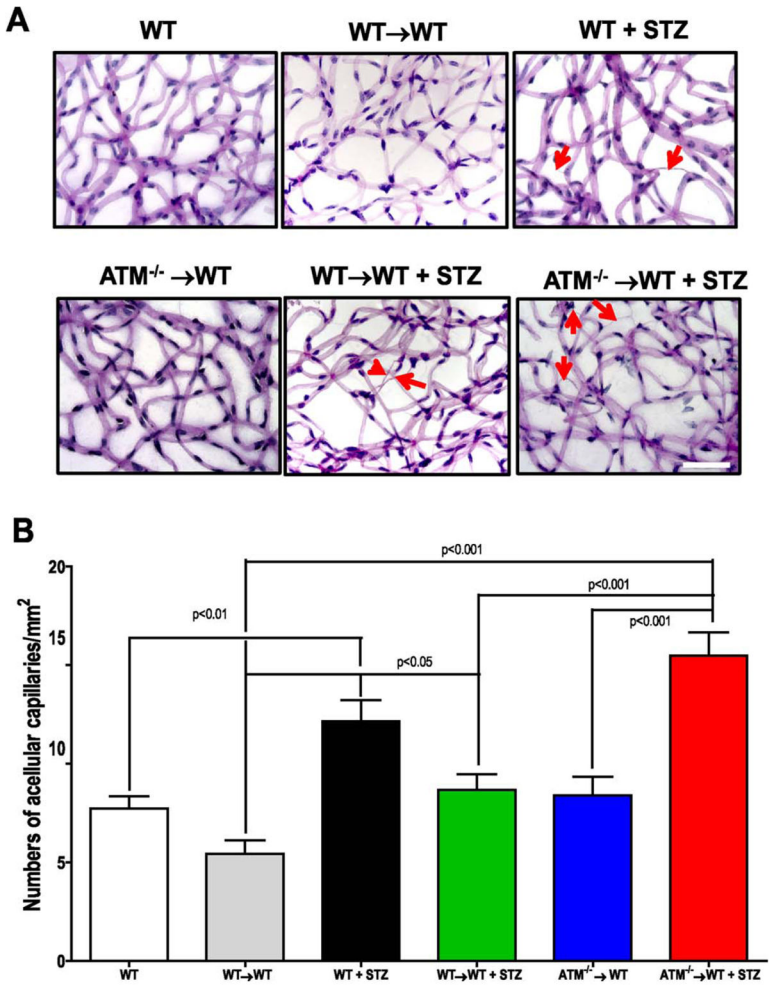

Figure 5.

Accelerated diabetic retinopathy (DR) in ataxia telangiectasia mutated $(ATM)^{-/-}\rightarrow$ wild type (WT) chimeras. **(A)**: Isolated mouse retinas were trypsin digested and stained with PAS-hematoxylin stain, top panel showing representative pictures of retinal trypsin digests from respective groups. Red arrows showing acellular capillaries as a marker of DR. Scale bar = 50 μm **(B)**: Bar chart showing quantification of numbers of acellular capillaries. WT (n = 6), WT→WT (n = 8) WT+ STZ (n = 5), $ATM^{-/-}\rightarrow$WT (n = 5) WT→WT + STZ (n = 9), $ATM^{-/-}\rightarrow$WT (n = 5) Statistical Test- One way analysis of variance followed by Student's Newman Keul Test. Abbreviations: ATM, ataxia telangiectasia mutated; STZ, streptozotocin; WT, wild type.

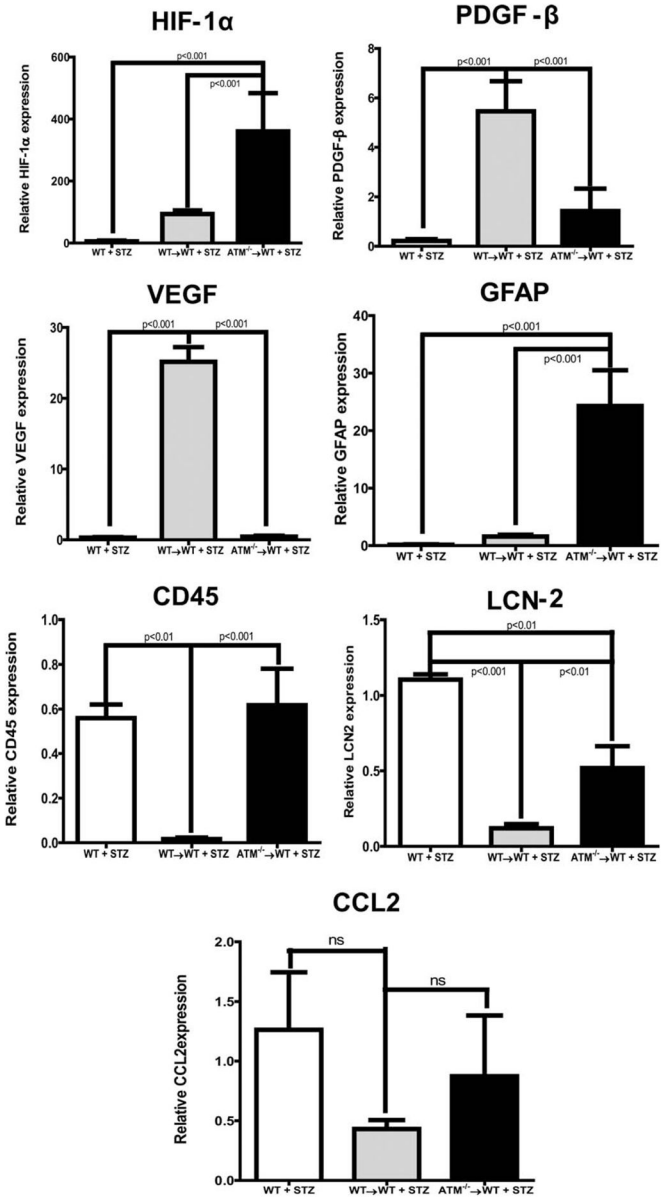

Figure 6.

Increase in retinal inflammation of ataxia telangiectasia mutated (ATM)$^{-/-}\rightarrow$ wild type (WT) chimeric animals. qRT-PCR was performed on isolated retinas, bar chart showing mRNA expression of a variety of retinal inflammatory markers (*HIF-1α, PDGF-β, vascular endothelial growth factor [VEGF], Glial fibrillary acidic protein [GFAP], CD45, Lipocalin-2 [LCN-2], and CCL2*). WT (n = 5), WT→WT (n = 8) WT+ STZ (n = 4), WT→WT + STZ (n = 13) ATM$^{-/-}\rightarrow$WT (n = 5), ATM$^{-/-}\rightarrow$WT (n = 5). Statistical test-one way analysis of variance followed by Student's Newman Keul Test. Abbreviations: ATM, ataxia telangiectasia mutated; CCL2, The chemokine (C-C motif) ligand 2; GFAP, Glial fibrillary acidic protein; HIF-1α, Hypoxia-inducible factor 1-alpha; LCN-2, Lipocalin-2; PDGF-β,

Platelet-Derived Growth Factor Beta; STZ, streptozotocin; VEGF, vascular endothelial growth factor; WT, wild type.

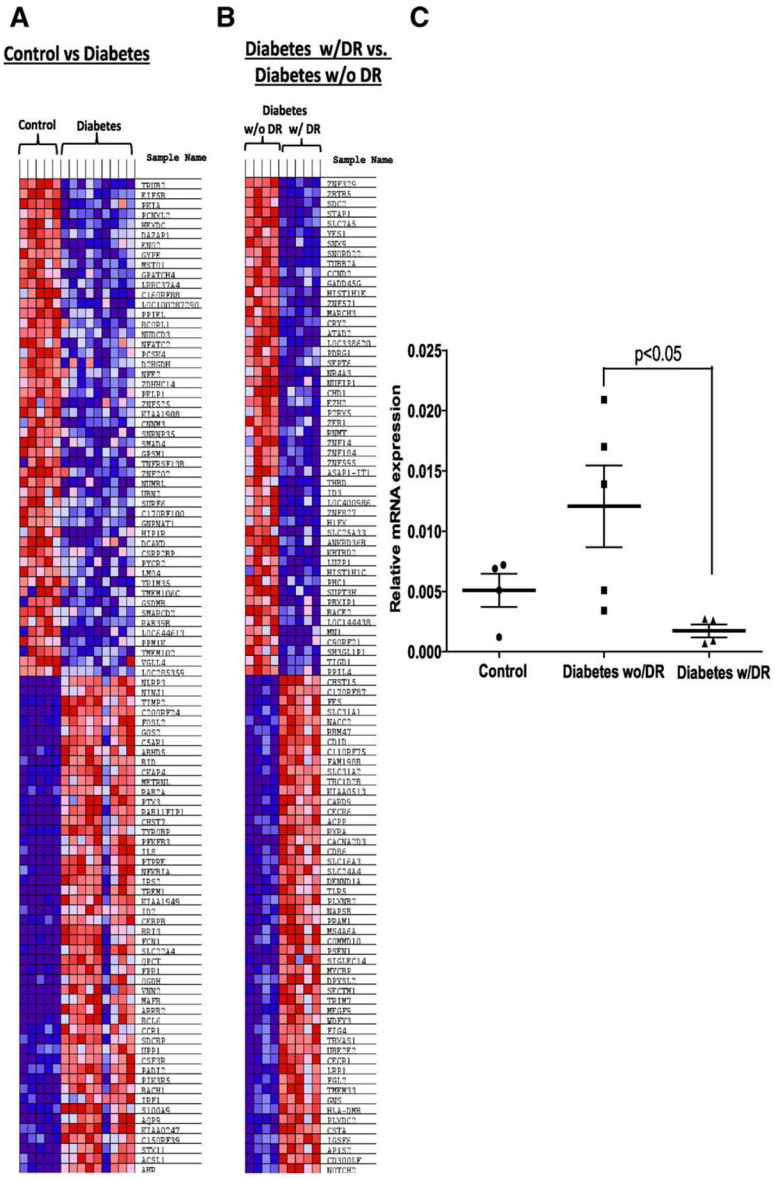

Figure 7.

Diabetic patients protected from microvascular complications map unique targets involved in DNA repair and cell cycle in $CD34^+$ cells. **(A)**: Gene set enrichment cluster analysis showing a heat map exhibiting distinct signature in diabetic group as compared with control. **(B)**: a similar comparison between protected patients from diabetic retinopathy (DR) and patients with DR. **(C)**: Dot plot showing mRNA expression of ataxia telangiectasia mutated in $CD34^+$ cells of study participants; Control ($n = 5$), Diabetes w/o DR ($n = 5$), Diabetes w/ DR ($n = 4$). Statistical test-one way analysis of variance followed by Student's Newman Keul Test. Abbreviation: DR, diabetic retinopathy.